JOURNAL OF GEOPHYSICAL RESEARCH, VOL. 110, B08203, doi:10.1029/2005JB003641, 2005

Morphometry of network and nonnetwork space of basins

L. Chockalingam
Faculty of Information Science and Technology, Melaka Campus, Multimedia University, Melaka, Malaysia

B. S. Daya Sagar
Faculty of Engineering and Technology, Melaka Campus, Multimedia University, Melaka, Malaysia

Received 22 January 2005; revised 18 March 2005; accepted 10 May 2005; published 11 August 2005.

[1] Morphometric analysis of channel network of a basin provides several scale-independent measures. To better characterize basin morphology, one requires, besides channel morphometric properties, scale-independent but shape-dependent measures to record the sensitive differences in the morphological organization of nonnetwork spaces. These spaces are planar forms of hillslopes or the retained portion after subtracting the channel network from the basin space. The principal aim of this paper is to focus on explaining the importance of alternative scale-independent but shape-dependent measures of nonnetwork spaces of basins. Toward this goal, we explore how mathematical morphology-based decomposition procedures can be used to derive basic measures required to quantify estimates, such as dimensionless power laws, that are useful to express the importance of characteristics of nonnetwork spaces via decomposition rules. We demonstrate our results through characterization of nonnetwork spaces of eight subbasins of the Gunung Ledang region of peninsular Malaysia. We decompose the nonnetwork spaces of eight fourth-order basins in a two-dimensional discrete space into simple nonoverlapping disks (NODs) of various sizes by employing morphological transformations. Furthermore, we show relationships between the dimensions estimated via morphometries of the network and their corresponding nonnetwork spaces. This study can be extended to characterize hillslope morphologies, where decomposition of three-dimensional hillslopes needs to be addressed.

Citation: Chockalingam, L., and B. S. Daya Sagar (2005), Morphometry of network and nonnetwork space of basins, *J. Geophys. Res.*, *110*, B08203, doi:10.1029/2005JB003641.

1. Introduction

[2] Characterization of branched networks, such as rivers, bronchial trees, vortex dynamic structures, and diffusion-limited aggregation to name a few, is one of the important research areas in geomorphology in recent decades. It is evident, from numerous studies, that various loopless networks ranging from geomorphologic [e.g., *Horton*, 1945; *Strahler*, 1957; *Mandelbrot*, 1982; *Turcotte*, 1997; *Rodriguez-Iturbe and Rinaldo*, 1997], physical [*Olson et al.*, 1998; *Mehta et al.*, 1999], and sociological networks [*Arenas et al.*, 2004] follow Hortonian laws. The Horton-Strahler morphometric statistics of networks that summarize the connectivity and orientation of convex zones of basins offer useful tools for quantitative description of landscapes. From the geophysical context, river networks are characterized via Hortonian laws and fractal-based power laws. Derivation of these laws based on stream number, mean stream length, and mean areas for river networks facilitates computation of topological quantities, such as bifurcation ratio (R_B), length ratio (R_L) and stream area ratio (R_A) as well as certain scaling laws to further validate and characterize numerous realistic and synthetic network [e.g., *Shreve*, 1967; *Mandelbrot*, 1982; *Tokunaga*, 1984; *LaBarbera and Rosso*, 1987; *Tarboton et al.*, 1988; *Takayasu*, 1990; *Howard*, 1990; *Marani et al.*, 1991; *Rigon et al.*, 1993; *Rinaldo et al.*, 1993; *Beer and Borgas*, 1993; *Nikora and Sapozhnikov*, 1993; *Kirchner*, 1993; *Karlinger et al.*, 1994; *Sagar*, 1996; *Maritan et al.*, 1996a, 1996b; *Rodriguez-Iturbe and Rinaldo*, 1997; *Turcotte*, 1997; *Sagar et al.*, 1998; *Peckham and Gupta*, 1999; *Sagar et al.*, 2001; *Gupta and Veitzer*, 2000; *Dodds and Rothman*, 2001; *Maritan et al.*, 2002; *Sagar and Tien*, 2004]. Geomorphic processes are explained by relation with the dimension, and certain scaling laws exhibited by networks.

[3] Besides channel network, nonnetwork spaces, the planar forms of hillslopes, are also important features within a basin. If the notion "geometry and topology of the basin have direct relationship with geomorphic processes" has merit, then scaling laws and dimension of the network are of limited use, as they enable less about the geometry and topology. Although, the organization of the network is strictly controlled by the spatial organization of concave zones, it is obvious that the Hortonian laws, which iron out much of the information, and scaling laws have emphasized

0148-0227/05/2005JB003641$09.00

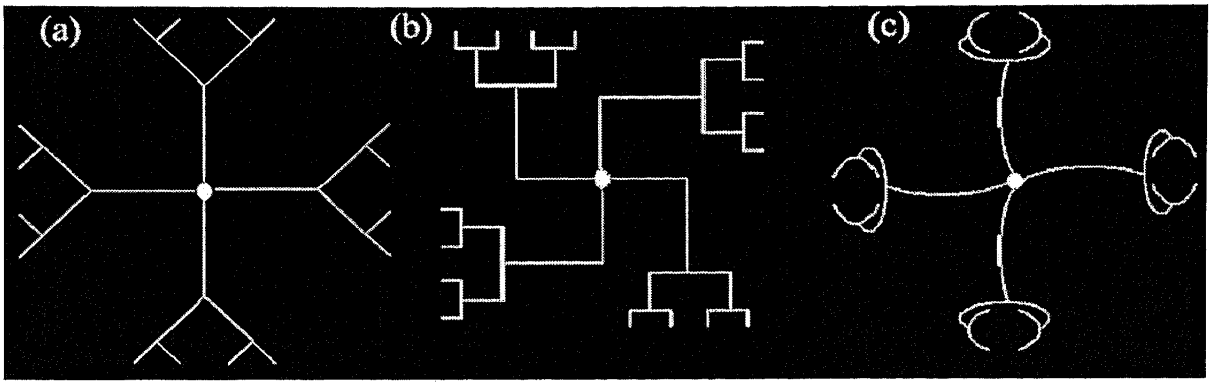

Figure 1. Schematically represented networks with three different geometric organizations.

only little on any shape-dependent quantity. Heuristically, similar networks that exist in an elongated and circular basins provide more or less similar Hortonion quantities. However, the processes involved, respectively, in elongated and circular basins differ significantly due to distinct geometries of nonnetwork space; in other words, planar forms of hillslope morphologies. We argue, as it is intuitively true, that network-based characteristics alone would be insufficient to quantify the sensible variations in the geometric and spatial organization of nonnetworks spaces, and to explore links with geomorphic expression and processes. To better explain this argument, we show three synthetic networks (Figure 1) with distinct topologies and geometric organizations of nonnetwork spaces, possessing similar laws of Horton's number and stream lengths. The typical difference between these three schematic networks (Figure 1) is obvious from the diverging angles between the segments and their overall geometry, and also the geometric organization of nonnetwork spaces. As the number of segments and their lengths of these three schematic networks, after designated with Horton-Strahler ordering scheme, are similar, the resultant topological quantities would also be similar. These similarities, irrespective of their dissimilarities in the topological organization of nonnetwork spaces, iron out much of the details.

[4] The quantitative description of concavity of the surface is done through the popularly known slope-area diagram [e.g., *Montgomery and Dietrich*, 1988, 1994; *Willgoose et al.*, 1991; *Tarboton and Bras*, 1992; *Moglen and Bras*, 1995; *Whipple and Tucker*, 1999]. Hillslopes, their morphologies and responses to changes in the tectonic and climatic settings were thoroughly investigated by numerous researchers to explore the characterization of hillslope morphologies via linear transport models [*Kirkby*, 1971; *Koons*, 1989; *Fernandes and Dietrich*, 1997] and nonlinear transport models [*Anderson*, 1994; *Howard*, 1994; *Roering et al.*, 1999]. Characterization of the planar form of hillslopes, which we term here as nonnetwork space, and its geometric composition enable rich clues to explore links with geomorphic processes within a basin. The topographically significant regions in the nonnetwork space include regions with varied degrees of slope, narrow regions with steep gradient, and the corner portions adjacent to the stream confluence.

[5] The components of the possible nonnetwork spaces, which may be isolated by subtracting the networks from their corresponding reconstructed basin, can be closely approximated with triangle, square and circle. We hypothesize that the geomorphic expression and activity depends upon the morphology of the components of nonnetwork spaces. Hence we propose morphometry of the nonnetwork space. We employ an elegant methodology, proposed by *Sagar and Chockalingam* [2004], whereby we derive shape-dependent dimensions, which consider the spatial organization of nonnetwork spaces that may be more relevant to relate with geomorphic processes that shape the basin.

[6] The paper is organized as follows. A brief outline of the basic morphological transformations used in implementation of procedures to isolate nonnetwork spaces from the reconstructed basins and to decompose the nonnetwork spaces into nonoverlapping disks (NODs) is presented in section 2. Then the results of our analysis on morphometry as applied to network and nonnetwork spaces of eight fourth-order basins of Gunung Ledang region are presented in section 3. We close by briefly discussing the implications of our results on morphologic characterization of networks and nonnetwork spaces in section 4.

2. Morphological Transformations, Nonnetwork Space Generation and Its Morphologic Decomposition

2.1. Basic Morphological Transformations

[7] We define channel network and nonnetwork spaces within a basin as if C in a two-dimensional Euclidean discrete space Z^2 belongs to the set A, the pixel representing channel network in the basin is white; otherwise it is black. The complement of channel networks (C^c) represents the channel network background. A symmetric template that performs various morphological transformations such as binary erosion, dilation, opening, and closing [*Serra*, 1982] at various phases of this investigation, is defined as follows: $S^s = [-s : s \in S\}$, where S^s is obtained by rotating S by 180° on the plane. Application of these transformations would be shown to reconstruct basins from channel networks and to decompose nonnetwork spaces into simpler convex components. We perform these transformations by

means of S that is symmetric with respect to the origin, octagonal in shape and has the size of 5 × 5.

[8] Erosion transformation of C by S expressed in equation (1) (denoted by $\ominus$) is defined as the set of three points c such that the translated S_c is contained in the original set C and is equivalent to intersection of all the translates:

$$C \ominus S = \{c : S_c \subseteq C\} = \bigcap_{s \in S} C_{-S}. \quad (1)$$

where for better legibility, this transformation is illustrated in matrix form (Figure 2a). In Figure 2a, a 3 × 3 size C is represented with 1 and 0 that stand for channel occupying and channel background regions, respectively. In Figures 2a and 2b, five channel points are obvious. These channel points are systematically translated in terms of symmetric S with characteristic information of size 3 × 3 and rhombus in shape as well as with center as origin. The number of translates required to achieve either erosion or dilation (Figures 2a and 2b) is equivalent to the number of channel points present. Hence five translates are required each for erosion and dilation. For the case of erosion, each channel point in C is systematically translated by means of S. The first translate is achieved in such a way that the origin in S (i.e., center point) is matched with the first encountered point of C at location (2, 1). This location depicts the second column of first scan line of C. Then we observe that S is not exactly overlapped with all the neighborhood channel points. Hence we consider this as "mismatch", and the first encountered channel point is transformed into channel background point. This is shown in the first translate involved in the erosion process. Similar translation is done for the second encountered channel point located at (1, 2) to check whether it exactly matches with S. As this second channel point also mismatches with reference to the origin of S, the second translate for channel point at location (1, 2) is transformed into channel background point. Similar exercise provides five translates as shown in Figure 2a. It is obvious that the translate achieved for the third encountered channel point at location (2, 2) exactly matches with S. Hence no change is observed in the corresponding translate. Further, the intersection of all the translates provides eroded version of C by S.

[9] Dilation transformation expressed in equation (2) (denoted by $\oplus$) of C by S is defined as the set of all those points c such that the translated S_c intersects C and is equivalent to the union of all translates:

$$C \oplus \mathrm{S} = \{c : S_c \cap C \neq \varnothing\} = \bigcup_{s \in S} C_{-S}. \quad (2)$$

The rule followed to translate the channel points to further achieve dilation is slightly different from the rule followed in erosion process. Here, while matching the first encountered channel point at location (2, 1) with reference to center point of S, we check for exact overlap with all points in S with all channel points. As for the first encountered channel point, we see that there is a mismatch. Then the points of S that are not exactly matched with channel points would be placed at locations beyond the channel points. This can be better comprehended from the first translate shown in Figure 2b. Similarly, the second and further translates are shown. As at the third encountered channel point the matching is exactly identified by means of S, there is no change observed in the corresponding translate. The union of all these translates produces dilated version of C by S as illustrated in matrix form (Figure 2b).

[10] The dilation with an elementary structuring template expands the set with a uniform layer of elements, while the erosion operator eliminates a layer from the set. To avoid confusion, $C \ominus S$ and $C \oplus S$ are simply referred to as erosion and dilation. Multiscale erosions and dilations are expressed as

$$(C \ominus S) \ominus S \ominus \ldots \ominus S = (C \ominus S_n) \quad (3)$$

$$(C \oplus S) \oplus S \oplus \ldots \oplus S = (C \oplus S_n), \quad (4)$$

respectively, where $S_n = S_1 \oplus S_2 \oplus \ldots \oplus S_n$. By employing erosion and dilation of C by S opening and closing transformations (denoted by $\circ$ and $\bullet$, respectively) are further represented as

$$C \circ S = ((C \ominus S) \oplus S)) \quad (5)$$

$$C \bullet S = ((C \oplus S) \ominus S)). \quad (6)$$

These transformations are illustrated in Figures 2c and 2d, where cascade of erosion followed by dilation of C of size 3 × 3 with nine channel points by means of S is shown. To perform erosion first on the nine channel points, nine translates are required. Then the resultant eroded version would be dilated to achieve the opened version of C by S as shown in Figure 2c. Similarly, to achieve closed version of C by S (Figure 2d), we first perform dilation on C of size 3 × 3 with nine channel points by means of S followed by erosion on the resultant dilated version. To perform these transformations shown in Figures 2a–2d, by changing the scale of S, one requires taking the addition of S by S to a desired level. As an example, we show in Figure 2e how we get S_2 by adding S_1 with S_1. We employ recursive erosions and dilations to perform multiscale opening and closing transformations in equations (7) and (8).

$$(C \circ S_n) = [(C \ominus S_n) \oplus S_n)] \quad (7)$$

$$(C \bullet S_n) = [(C \oplus S_n) \ominus S_n)], \quad (8)$$

where n is the number of times the transformations are repeated. We encourage the reader to refer to *Matheron* [1975] and *Serra* [1982] for morphological transformations and their numerous applications. These transformations are employed systematically (Figure 3) as explained in the equations to first achieve the reconstructed basin space (X) from channel network (C) and then to generate nonnetwork space (M). Once M is achieved, we employ these

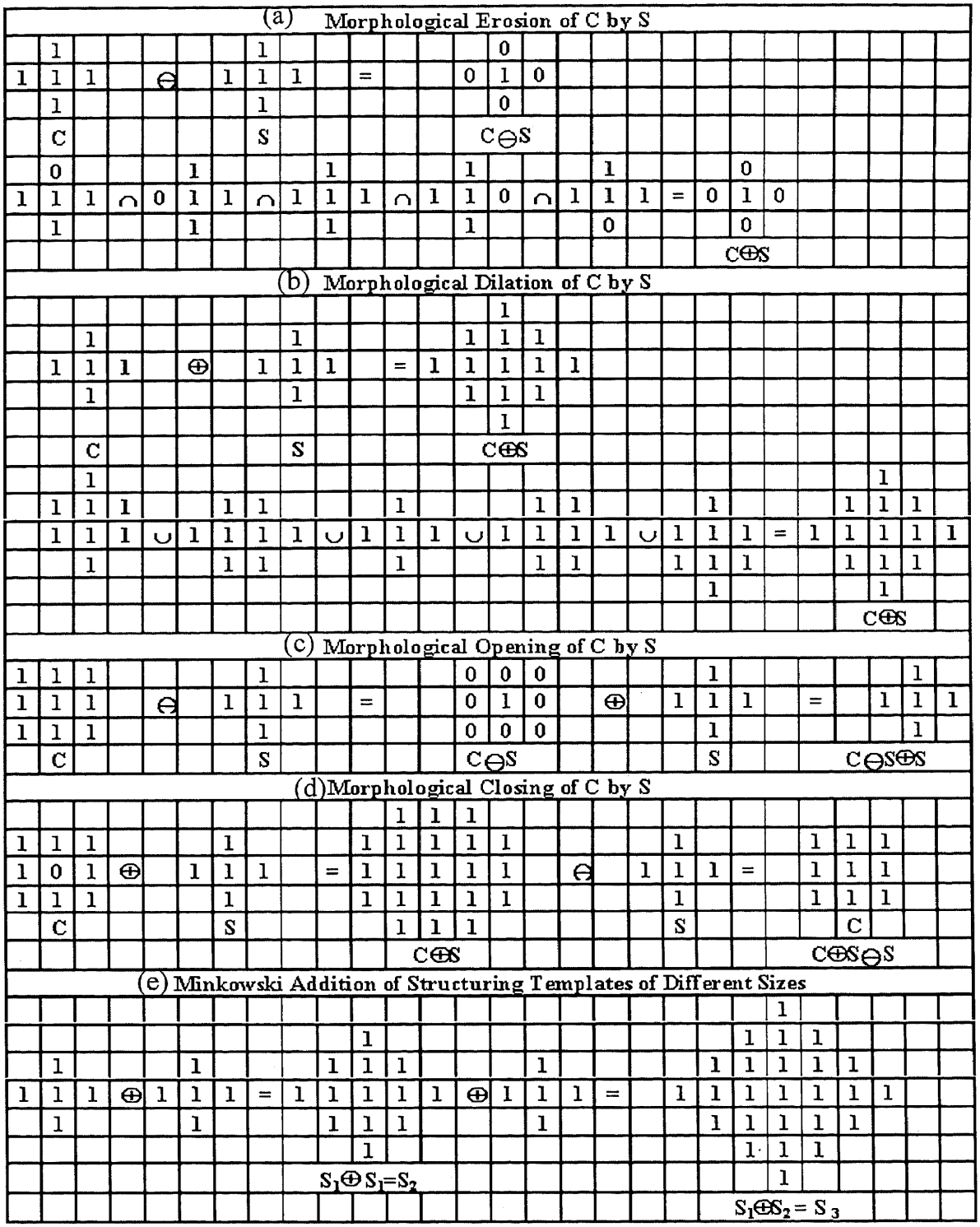

Figure 2. Matrix representations of morphological transformations and certain logical operations. (a) Morphological erosion and involved translates, (b) dilation and involved translates, (c) opening, (d) closing, and (e) structuring templates of varied sizes and their Minkowski additions. Refer to text for detailed explanation. See color version of this figure in the HTML.

transformations again to convert M into nonoverlapping disks (NODs), which are simpler convex components. We replace C with M. One can perform these transformations also on nonnetwork space.

2.2. Nonnetwork Space of Basins

[11] The landscape of a part of Gunung Ledang region (Figure 4), situated between 02°21′–02°27′N latitude and 102°35′–102°41′E longitude, with varied topographic

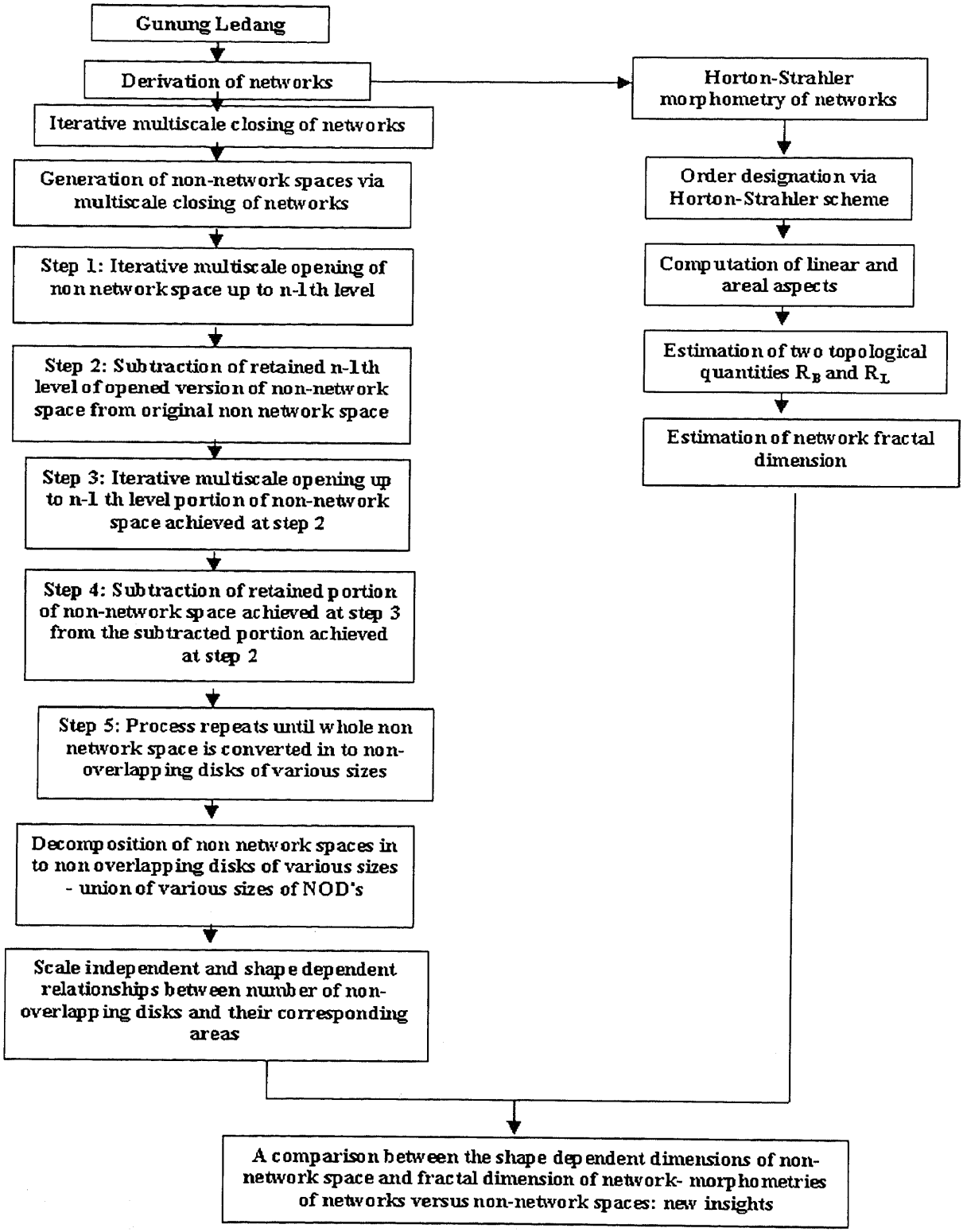

Figure 3. Flowchart showing sequential steps involved in derivation of nonnetwork space-based shape-dependent dimensions of eight subbasins of Gunung Ledang region and their comparison with network-based morphometric parameters.

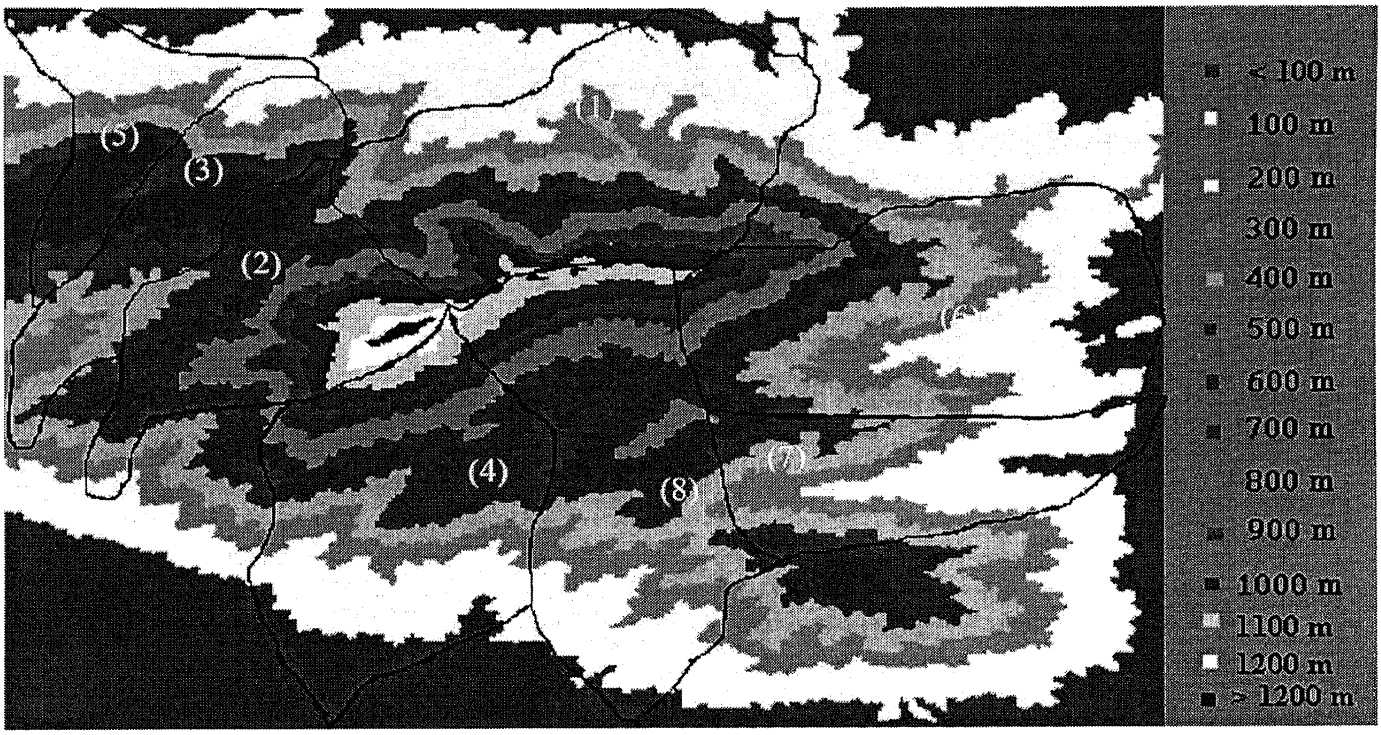

Figure 4. Gunung Ledang DEM after partitioning into eight fourth-order basins. See color version of this figure in the HTML.

relief, consisting of eight fourth-order basins of several sizes and shapes, is considered in the present study. The Gunung Ledang forested mountainous landscape region is tropical, being characterized by fairly uniform high temperatures, high humidity and fairly heavy rainfall, and is occupied with granite massif that projects above the surrounding undulation, low-lying sedimentary and pyroclastic rocks. The observed drainage patterns include trellis and radial type. Our investigation of nonnetwork spaces is motivated by these observations from the Gunung Ledang region, although this methodology can be applied to any nonnetwork space.

[12] The channel connectivity networks (Figure 5) derived from eight basins are illustrated with Horton-Strahler ordering scheme. The spatial organization of these network patterns determines the basin processes. We employ these channel networks to reconstruct the basins with proper characteristics. A framework (Figure 3) based on morphological transformations due to *Sagar and Chockalingam* [2004] is employed to reconstruct the basins and their internal topological organizations. From such a reconstructed basin, it is also possible to attain a network much similar to the network that is used to reconstruct the basin.

[13] To reconstruct the basin and its topology from channel network, we let C be the channel network (Figure 5) and a discrete probing rule, with $S \in Z^2$ (e.g., Figure 2e), bounded, convex, symmetric and containing the origin. Channel networks and their complementary spaces are represented with white and black pixels, respectively. To reconstruct the basins from channel networks, we employ multiscale closing as expressed in equation (9).

$$X = \bigcup_{n=0}^{N} C \bullet S_n, \tag{9}$$

where $C \subset X$, C and X are channel network and basin reconstructed from channel network by performing multiscale morphological closing transformation iteratively until X becomes equivalent to $X \bullet S_1$; in other words, the closure of the closure of a set X is equal to the closure of that set. Channel networks are subtracted from the reconstructed basins to achieve nonnetwork spaces within basins. We define nonnetwork space (M) within each reconstructed basin (X) as a combination of disconnected, bounded, binary valued discrete space object as depicted

$$M = [X \backslash C] \subset Z^2, \tag{10}$$

where reverse slash denotes subtraction. By subtracting the channel networks from the bounded reconstructed basins X, we obtain nonnetwork spaces M (Figure 6) of the eight basins. For better understanding of basin reconstruction process from the network, we show an evolutionary sequence of network for basin 1 after respective multiscale closings in the inset picture (Figure 6). The nonnetwork space (M) is similar to the nonchannelized convex region that consists of varied degrees of topographically convex regions within a basin. As an extension, we emphasize on characterization of nonnetwork spaces of the eight basins by involving decomposition rules that are similar to random

Figure 5. Fourth-order channel networks of eight basins of Gunung Ledang region. See color version of this figure in the HTML.

packing of space, reported elsewhere [*Manna and Herrmann*, 1991; *Dodds and Weitz*, 2002, 2003; *Lian et al.*, 2004; *Radhakrishnan et al.*, 2004]. Decomposition of these nonnetwork spaces into nonoverlapping disks (NODs) of various sizes such that the nonnetwork space within each is filled with NODs of decreasing sizes provides valuable insight for modeling and understanding basins. The characterization of such a scale-dependent topological organization of nonnetwork space has hitherto been received little attention.

2.3. Morphological Decomposition of Nonnetwork Space

[14] Complex nonnetwork spaces (M) of eight basins are transformed into "simpler convex polygon-like" NODs. A symmetric octagonal structuring element, as a simple probing rule, is considered to convert M into NODs by employing morphological decomposition according to the following recursive relation. Three steps involved in recursive relation:

$$\begin{aligned} &\text{Step 1} \quad M_i = \left[\left(M - M'_{i-1}\right) \ominus S_{n_i}\right] \oplus S_{n_i}, \\ &\text{Step 2} \quad M'_i = \bigcup_{0<j\le i} M_j, \\ &\text{Step 3} \quad M'_0 = \phi, \end{aligned} \tag{11}$$

where n_i denotes the maximal size of the maximum inscribable disks S_{ni} in any of the connected components of $M - M'_{i-1}$. The description of the above equation with

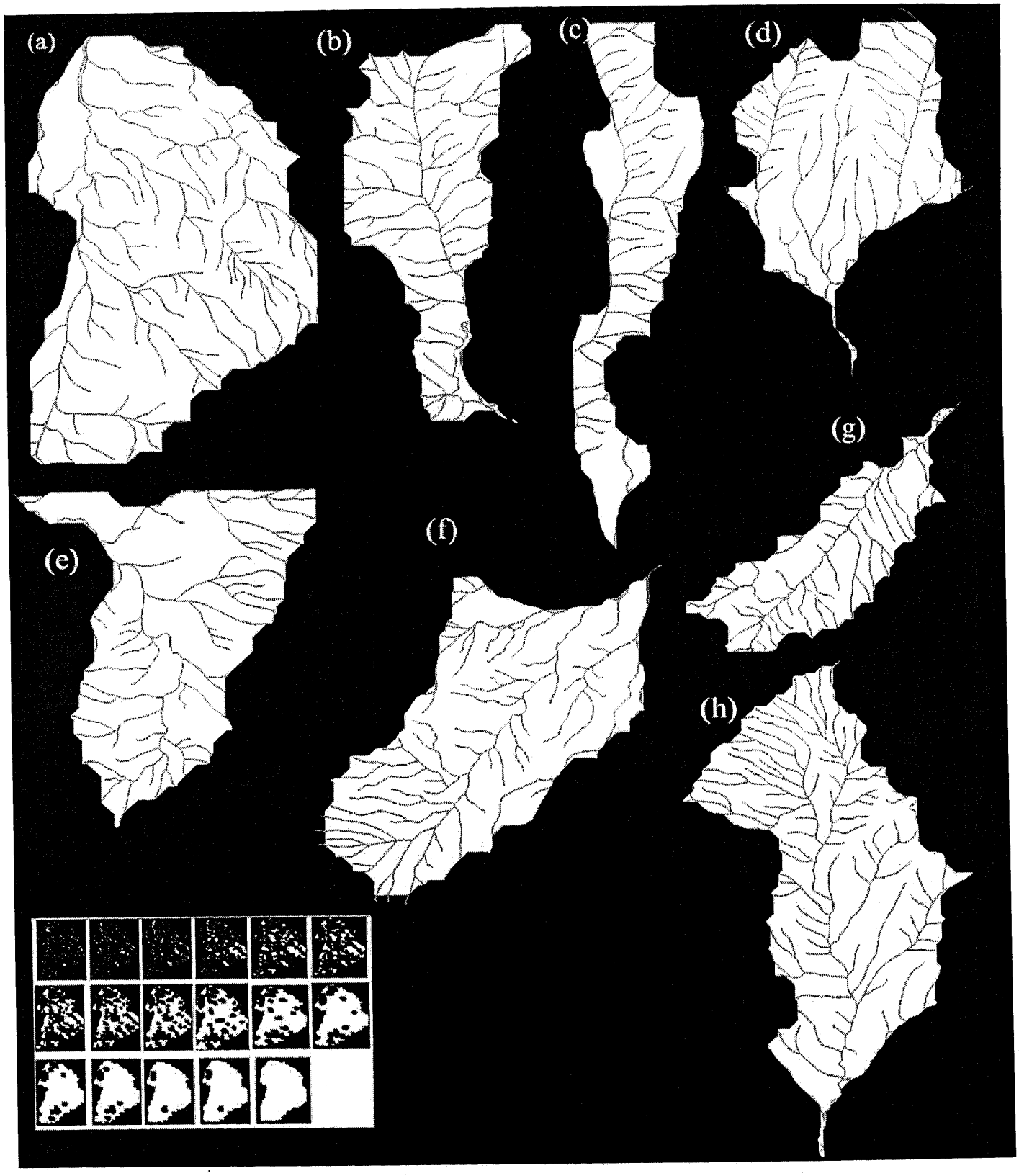

Figure 6. $M = X \backslash C$ is nonnetwork space in white and networks in black within a basin. For basin reconstruction stages, we explain with reference to first basin. A similar approach has been followed to generate topological spaces within the other seven basins. Evolution of networks of first basin after respective multiscale closings is shown in inset.

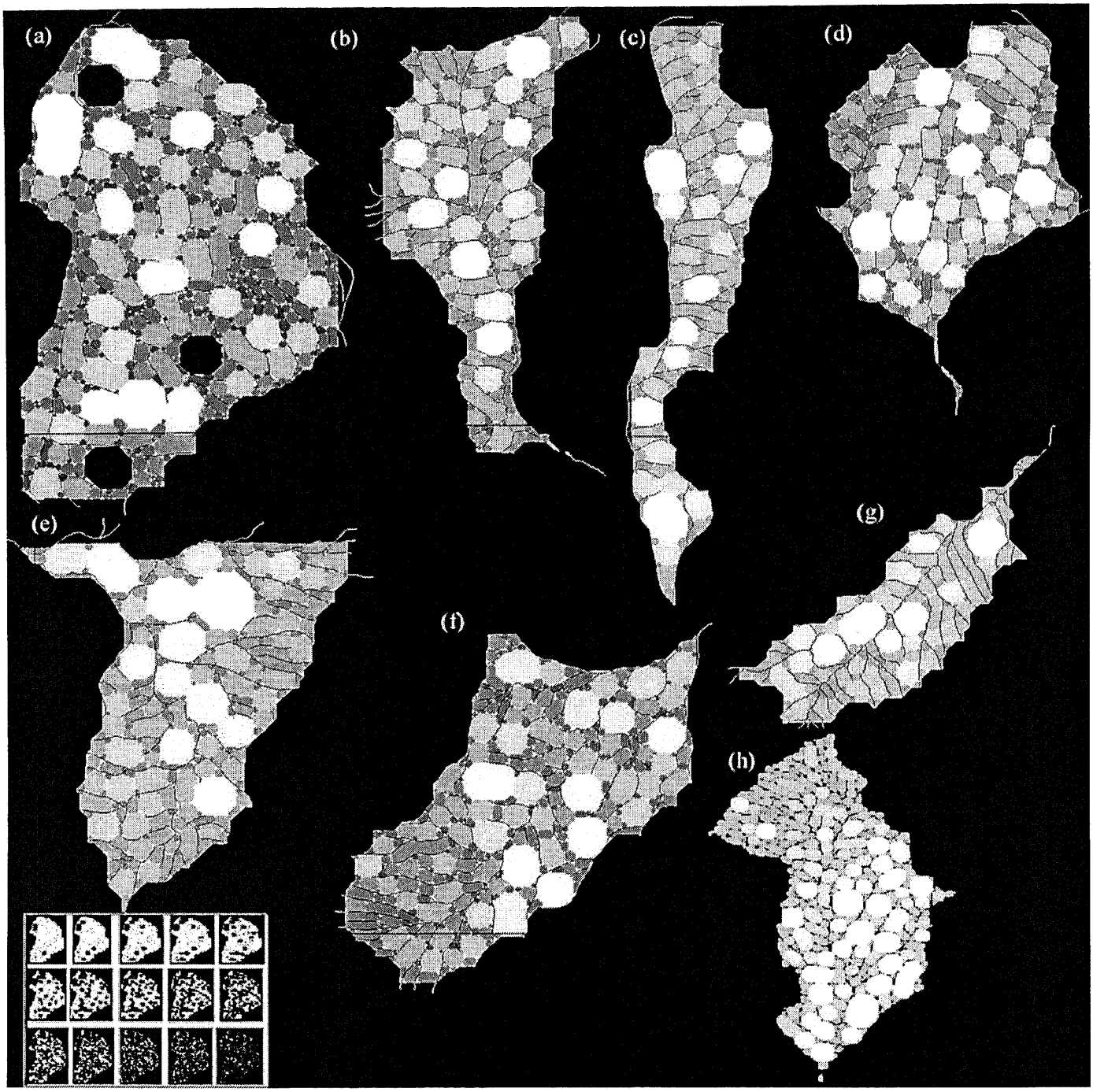

Figure 7. Nonnetwork spaces of eight basins after filling with nonoverlapping octagons of several sizes. Evolution of decay of nonnetwork space of first basin into nonoverlapping disks of decreasing sizes is shown as an inset picture.

three steps involved in morphological decomposition of nonnetwork space of the basin into NODs includes obtaining the set of maximum inscribable disk(s) that has (have) the maximum radius in M. This set is the first level decomposed disk(s) in the decomposition. The second set of the maximum inscribable disks in the portion of the basin is that obtained by subtracting the first cluster from M. The procedure is repeated on the portion of each basin that is obtained by subtracting the first and second decomposed disks, until the remainder of the nonnetwork space becomes an empty set. The more regular is the set M, the smaller is the number of categories of regular type NODs of different sizes. Here, we decompose the space in a nonoverlapping manner with an octagon. The shape, size, orientation, and origin of S can be changed to unravel various other topological characteristics of nonnetwork spaces of basins.

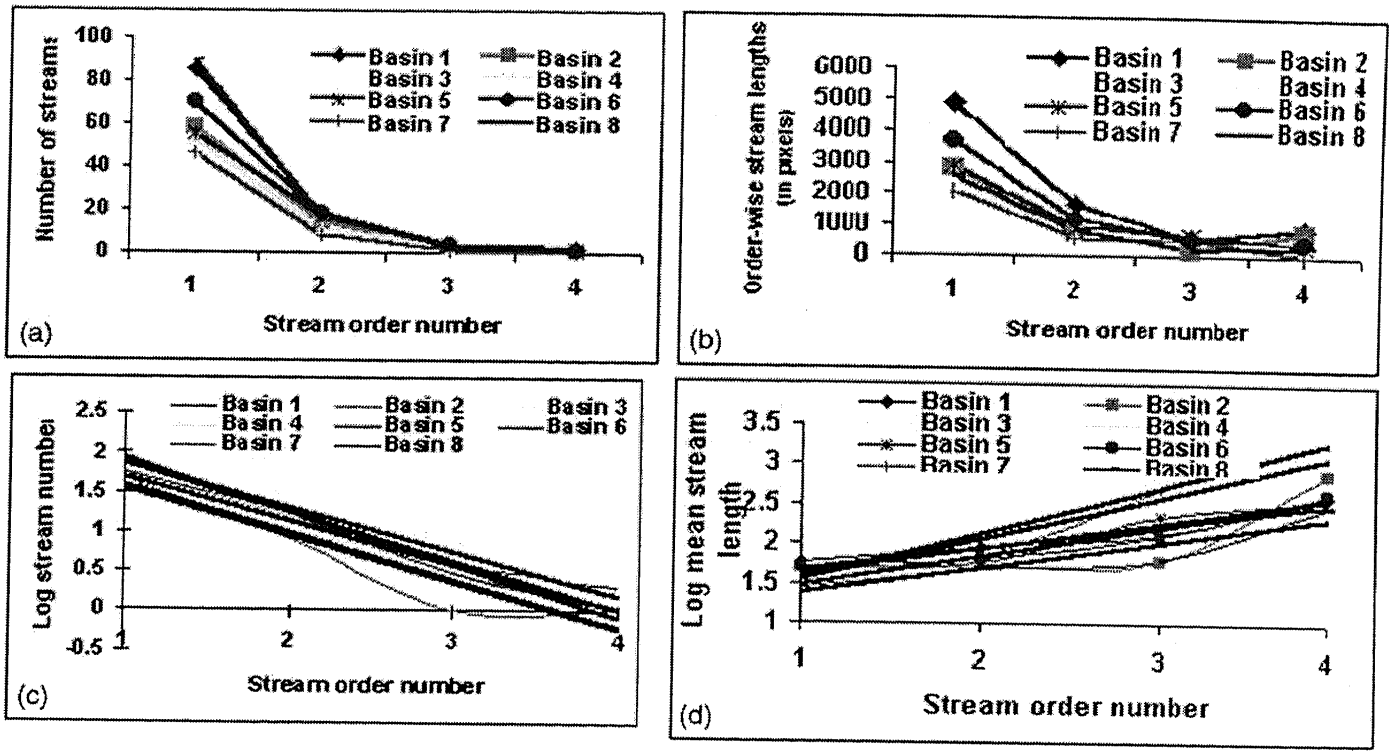

Figure 8. (a, b) Graphical plots between stream order and order-wise stream number and lengths and (c, d) stream orders versus logarithms of order-wise numbers, and mean stream lengths of eight basins. See color version of this figure in the HTML.

The nonoverlapping disks $[M_1, \ldots, M_n]$ whose union is M, is depicted

$$M = \bigcup_{i=1}^{n} M_i, \tag{12}$$

where M_i is a simple set that is equal to discrete rule S of size r_i : $M_i = S_{ri}$, where r_i is the same integer as in the relation $M_i = S \oplus S \oplus \ldots \oplus S$ (n times, where circled cross denotes Minkowski addition; see Figure 2e). Figure 7 illustrates the decomposition of nonnetwork spaces of eight basins into NODs explained in sequential phases. For better legibility, each category of NODs is coded with gray shades. These NODs, corresponding to each basin achieved through morphological decomposition procedure, are considered to quantify the geometric complexities of nonnetwork spaces. Nonnetwork spaces of each basin consist of several isolated connected components, which are the planar forms of hillslopes within a basin. It is obvious that the nonconvex connected components consist of more size categories of NODs than that of convex connected components.

3. Morphometry of Network and Nonnetwork Space of Eight Basins of Gunung Ledang Region

[15] In this section, we provide morphometric parameters of both network and nonnetwork spaces of eight basins.

3.1. Morphometry of Networks

[16] Eight subbasins are derived from the hilly Gunung Ledang region of Malaysia. The channel networks within these basins are traced and designated the stream ordering according to Horton-Strahler scheme. The order-wise number of streams and their lengths in pixel units are computed (Table 1). Figures 8a and 8b depict graphical relationships between the stream order and order-wise stream numbers and lengths. Graphical plots between the stream orders and logarithms of order-wise stream lengths and numbers for all the eight basins (Figures 6c and 6d) facilitate computations of bifurcation and stream length ratios (Table 1). Order-wise stream numbers and lengths are plotted as functions of stream orders for eight fourth-order networks of the Gunung Ledang region. Linear relationships are observed for logarithms of mean stream lengths and number plotted as functions of stream orders. These linearities indicate Hortonity of the networks. From these linear relationships, we derive Hortonian laws of stream lengths and numbers. We compute the antilogarithms of absolute slope values computed from these linear relationships that represent basin-wise bifurcation (R_B) and stream length (R_L) ratios, respectively, for the eight basins (Table 1). Basin 7 possesses the highest bifurcation ratio followed by basins 3, 8 and 6, indicating that the underlain geological structures disturb the stream networks relatively lesser than that of other basins 2, 5, 4 and 1. Estimated higher fractal dimensions for basins 8, 6, 4, and 5 indicate higher degrees of space-filling characteristics. We infer that these dimensions derived from morphometry of networks explain space-filling characteristics of networks. However, these measures offer little scope to quantify the geometric complexity of hillslopes. On the basis of the morphometric statistics of the eight networks, the networks' complexity is in ascending

Table 1. Basic Measures of Networks of Eight Basins

	Order				Stream Length, pixels					
Basin	1	2	3	4	1	2	3	4	R_B	R_L
1	85	18	4	2	4891	1611	551	849	3.45	1.90
2	58	15	3	1	2818	775	187	767	3.97	2.33
3	45	11	1	0	2346	594	770	0	6.64	3.87
4	53	11	4	1	2789	748	703	328	3.64	1.90
5	55	17	3	1	2834	961	659	374	3.96	2.07
6	70	18	4	1	3671	1182	518	431	4.16	2.01
7	46	8	1	0	2042	562	479	0	6.78	3.28
8	89	17	3	1	2477	809	194	294	4.57	2.09

order for the basins 3, 7, 2, 5, 1, 4, 6, and 8. We demonstrate, on the basis of the arguments made with reference to Hortonically similar synthetic networks (Figures 1a–1c), that the characterization of nonnetwork spaces through statistical relationships of NOD' statistics would provide geometric-dependent complexity measures.

3.2. Morphometry of Nonnetwork Spaces

[17] The geometric complexity of nonnetwork spaces that are computed via fragmentation rules provides four different shape-based measures. We record the number of decomposed nonoverlapping disks, of sizes lesser than the template of specific radius, and their contributing area in pixels (Table 2). The statistics of NODs of various sizes that reveal other interesting characteristics for the eight nonnetwork spaces include number of NODs and their contributing areas. We observe that more number of smaller size category NODs exist in the eight basins. Decay in the number of NODs in these basins is obvious (Figure 9a). Similarly the distributary patterns in the contributing areas of size-wise NODs for these eight basins (Figure 9b) show significant oscillations indicating different NOD size categories, which are less in number, occupying larger contributing areas.

[18] The largest templates that could be fit in the eight basins ranging from the first to the eighth basins are of the radii of 32, 28, 26, 26, 34, 26, 24, and 26 pixels, respectively (Table 2). We estimate the fractal dimension of the nonnetwork space through the following steps. We determine power law exponents for the NODs' number and size distributions by means of a connection to the decay of nonnetwork space of basin. On the basis of the assumption that the shape of the nonnetwork space alters the number and size distributions of NODs, these exponents are strongly shape-dependent. We compute the number of NODs smaller than the specified threshold radius of the structuring template and their contributing areas (Table 3) denoted as $N[\text{NODs } (<S_{n_1})]$ and $A[\text{NODs}(<S_{n_1})]$, respectively. The distribution of number and area of nonoverlapping disks, decomposed from nonnetwork space, depends on the diverging angles of streams. The rate at which the nonnetwork space within a basin gets decayed via morphological decomposition depends on the area, geometric organization, and the outline roughness of connected components of nonnetwork space. We propose that the dimensions derived from analysis of nonnetwork space provide better reasons to explore links with processes and geomorphic expression of the basin than that of network morphometric characteristics. By employing the numbers of NODs of various sizes, their contributing areas, and the corresponding radius of template, we derive simple power law relationships for these eight realistic basins. Figures 9c–9j show double logarithmic graphs for the cumulative number of NODs (diamonds) smaller than the threshold radius of the structuring template (disk) and their corresponding contributing areas (squares) versus the radii of structuring elements n. The slopes of the best fit lines (α_N and α_A) for number-radius and area-radius relationships, respectively (Table 4) (Figures 9c–9j), are obtained from the well fitted relationships as $N[\text{NODs}(<S_{n_1})]$ or $A[\text{NODs}\{<S_{n_1})] \sim n^{\alpha_N \text{ (or) } \alpha_A}$, where n is radius of template, and α is slope of the best fit line. These slope values of the best fit lines provide shape-dependent dimensions as $D_N =$

Table 2. Basic Statistics of Distributed Number of Nonoverlapping Disks and Their Contributing Areas of Various Sizes Decomposed From Nonnetwork Space of Eight Basins[a]

Disk	N								A							
Size	1	2	3	4	5	6	7	8	1	2	3	4	5	6	7	8
1	247	139	88	136	148	167	79	197	13201	7300	4863	7642	7985	9404	4778	10011
2	88	50	38	48	50	56	32	81	11358	7280	5416	6228	7395	8267	4080	12807
3	53	23	19	27	41	48	27	56	15444	6198	4231	8609	11946	13936	8254	18218
4	35	18	13	19	19	31	15	36	13888	8630	5237	7858	7831	13460	6004	14990
5	28	19	14	18	14	13	13	24	13785	13083	10164	10304	8496	7772	7814	16167
6	11	9	12	12	12	18	4	12	11648	6697	9924	11033	10710	14843	4277	8743
7	19	7	7	11	8	12	4	12	23316	7778	7421	11195	7484	12396	3836	11741
8	8	7	4	7	7	5	1	11	12216	8143	4646	8350	7630	5404	945	16512
9	11	3	5	3	4	3	0	3	18416	4802	7455	4197	6020	4271	0	4538
10	9	3	0	2	3	4	2	4	16468	5276	0	3715	5815	7243	3453	6743
11	5	2	1	3	2	4	1	2	13918	3702	2083	6639	4199	12777	3075	4067
12	2	0	0	1	2	4	1	1	4337	0	0	2834	4475	10031	2360	3446
13	2	1	2	1	2	2	0	1	8160	2445	6711	2753	7159	5978	0	2632
14	0	1	0	0	2	0	0	0	0	3339	0	0	5916	0	0	0
15	0	0	0	0	0	0	0	0	0	0	0	0	0	0	0	0
16	2	0	0	0	1	0	0	0	5859	0	0	0	3681	0	0	0
19	0	0	0	0	1	0	0	0	0	0	0	0	2407	0	0	0

[a] N is number of respective stream orders.

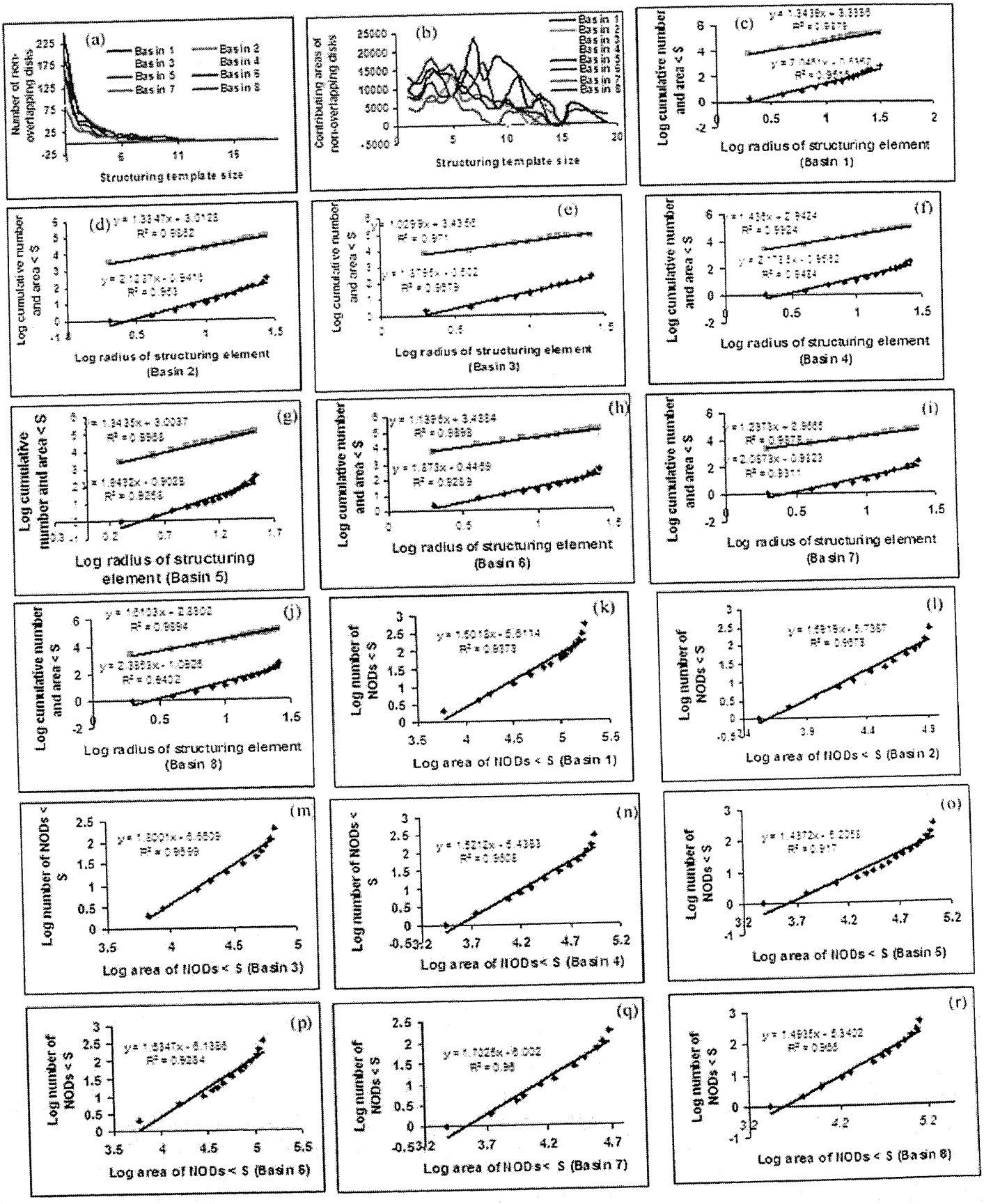
(a)
Number of non-overlapping disks
Structuring template size
Basin 1
Basin 2
Basin 3
Basin 4
Basin 5
Basin 6
Basin 7
Basin 8
(b)
Contributing areas of non-overlapping disks
Structuring template size
(c)
Log cumulative number and area < S
Log radius of structuring element (Basin 1)
(d)
Log cumulative number and area < S
Log radius of structuring element (Basin 2)
(e)
Log cumulative number and area < S
Log radius of structuring element (Basin 3)
(f)
Log cumulative number and area < S
Log radius of structuring element (Basin 4)
(g)
Log cumulative number and area < S
Log radius of structuring element (Basin 5)
(h)
Log cumulative number and area < S
Log radius of structuring element (Basin 6)
(i)
Log cumulative number and area < S
Log radius of structuring element (Basin 7)
(j)
Log cumulative number and area < S
Log radius of structuring element (Basin 8)
(k)
Log number of NODs < S
Log area of NODs < S (Basin 1)
(l)
Log number of NODs < S
Log area of NODs < S (Basin 2)
(m)
Log number of NODs < S
Log area of NODs < S (Basin 3)
(n)
Log number of NODs < S
Log area of NODs < S (Basin 4)
(o)
Log number of NODs < S
Log area of NODs < S (Basin 5)
(p)
Log number of NODs < S
Log area of NODs < S (Basin 6)
(q)
Log number of NODs < S
Log area of NODs < S (Basin 7)
(r)
Log number of NODs < S
Log area of NODs < S (Basin 8)

Figure 9

Table 3. Cumulative Number and Corresponding Contributing Areas of Nonoverlapping Disks of Various Sizes Decomposed From Nonnetwork Space of Eight Basins[a]

	Basin															
	1		2		3		4		5		6		7		8	
SE	*N*	*A*	*N*	*A*	*N*	*A*	*N*	*A*	*N*	*A*	*N*	*A*	*N*	*A*	*N*	*A*
34	-	-	-	-	-	-	-	-	316	109149	-	-	-	-	-	-
32	520	182014	-	-	-	-	-	-	168	101164	-	-	-	-	-	-
30	273	168813	-	-	-	-	-	-	118	93769	-	-	-	-	-	-
28	273	168813	282	84673	-	-	-	-	118	93769	-	-	-	-	-	-
26	273	168813	143	77373	203	68151	288	91357	77	81823	367	125782	-	-	440	130615
24	185	157455	93	70093	115	63288	152	83715	58	73992	200	116378	179	48876	243	120604
22	132	142011	93	70093	115	63288	104	77487	44	65496	144	108111	100	44098	162	107797
20	97	128123	70	63895	77	57872	77	68878	32	54786	96	94175	68	40018	106	89579
18	69	114338	52	55265	77	57872	58	61020	24	47302	65	80715	41	31764	70	74589
16	58	102690	33	42182	58	53641	40	50716	17	39672	52	72943	41	31764	46	58422
14	39	79374	24	35485	45	48404	28	39683	13	33652	34	58100	26	25760	34	49679
12	31	67158	17	27707	31	38240	17	28488	10	27837	22	45704	13	17946	22	37938
10	20	48742	10	19564	19	28316	10	20138	8	23638	17	40300	9	13669	11	21426
8	11	32274	7	14762	12	20895	7	15941	6	19163	14	36029	5	9833	8	16888
6	6	18356	4	9486	8	16249	5	12226	4	12004	10	28786	4	8888	4	10145
4	4	14019	2	5784	3	8794	2	5587	2	6088	6	16009	2	5435	2	6078
2	2	5859	1	3339	2	6711	1	2753	1	2407	2	5978	1	2360	1	2632

[a]SE is structuring element, *A* is area in pixel units, and *N* is number of NODs.

$\alpha_N - 1$, and $D_A = \alpha_A$ yield D_N and D_A for nonnetwork spaces of eight basins. The slopes are under 1.61 for the number of NODs, and are under 2.38 for the contributing areas of NODs. These slope values can be related with erosion laws. These relations can also be linked with slope-area diagram. These statistically derived measures are dependent upon characteristic information of template used to convert the nonnetwork spaces into NODs. The third measure is derived from the plots made by considering the number of NODs as functions of their corresponding areas. The geometric complexities for these eight networks, computed by taking the contributing areas of NODs as functions of radii of templates, are in the ascending order for the basins 3, 6, 7, 2, 1, 5, 4, and 8. It is obvious, from the comparison, that there is no relation between network-based topologic quantities and nonnetwork-based complexity measures. In addition to these statistically derived power law relationships for nonnetwork spaces, we also derive shape-based complexity measures by estimating uncertainty index for the number of NODs and their areas. The NODs of various sizes are categorized according to their sizes by performing opening with increasing cycles. For instance, the NODs of nonnetwork space of first basin are segregated into 16 size categories. The distributions of the number of NODs and their contributing areas are computed for these eight basins (Table 2). We employ these basic measures of size distributed NODs to estimate probability distribution functions of number and area (Table 4). By employing these normalized plots of number and area, we estimate complexity measures (Table 4) by following entropy equations

$$H(N)/M = -\sum_{n=1}^{19} p_N(n)\log[p_N(n)]$$

$$H(A)/M = -\sum_{n=1}^{19} p_A(n)\log[p_A(n)],$$

where p_N, p_A, $H(N)/M$, and $H(A)/M$ denote probability distribution functions and average uncertainty indexes for the number of NODs and their areas, respectively. These measures are also scale-independent and shape-dependent that quantify the degree of randomness in the distributions of the number of NODs and their corresponding areas.

[19] For the considered eight subbasins, we show these shape-dependent and nonshape-dependent dimensions derived from the nonnetwork spaces and network morphometries of eight basins, respectively (Figure 10). Characterization of network via nonshape-dependent morphometric parameters is not sensitive to sinuosity of stream segments. However, the nonnetwork space characterized via dimensions is sensitive to sinuosity of network (or) curvature and geometric organization of space occupied by varied degrees of convex region within a basin. On the other hand, the

Figure 9. Morphometric parameter computations achieved through decomposition of nonnetwork space. (a, b) Numbers of NODs of nonnetwork spaces and their corresponding areas as functions of radius of structuring element for considered nonnetwork spaces of eight basins, (c–j) double logarithmic relationships between the radius of template and number of NODs and their contributing areas lesser than the radius of template for eight basins, and (k–r) areas of NODs and number of NODs lesser than the template. The points of these graphs organize themselves into a straight line, the slopes of which for these basins characterize nonnetwork spaces of basins. See color version of this figure in the HTML.

Table 4. Dimensions Derived From Morphometry of Network and Power Laws Derived From Nonoverlapping Disks of Nonnetwork Space and Shape Complexity Measures Estimated for NODs Number and Their Corresponding Areas[a]

	Network		Nonnetwork Space				
Basin	Network FD	(log R_B/log R_L)	R versus A	R versus N	A versus N	$H(N)/M$	$H(A)/M$
1	1.83	1.93	1.34	2.04	1.50	0.76	1.116
2	0.86	1.63	1.33	1.23	1.59	0.73	1.078
3	0.98	1.41	1.02	1.87	1.80	0.77	1.009
4	2.07	2.01	1.43	2.17	1.52	0.75	1.075
5	1.73	1.90	1.34	1.94	1.43	0.76	1.108
6	1.84	2.04	1.13	1.87	1.63	0.77	1.086
7	1.33	1.61	1.23	2.08	1.70	0.72	0.991
8	1.65	2.06	1.61	2.38	1.49	0.74	1.050

[a]FD is fractals dimension; R_B is bifurcation ratio; R_L is stream length ratio; R is radius of structuring element; N is number of NODs.

dimensions derived from their corresponding nonnetwork spaces are shape-dependent.

4. Conclusions

[20] This paper addresses four aspects: (1) reconstruction of the basin from channel networks, (2) generation of nonnetwork spaces (M) from the basins (X) reconstructed from channel network such that the channel networks are contained in X, (3) decomposition of M into NODs to compute morphometry of nonnetwork spaces, and (4) derivation of relationships among several parameters of morphometries of networks and their nonnetwork spaces. To achieve these, we use set theory and topology-based mathematical transformations that have hitherto been relatively less employed in geophysics. This framework and the results derived from realistic cases allow systematic characterization and validation of the topological properties of the nonnetwork space of various realistic and simulated networks via shape-dependent measures. This systematic framework to quantify the organization of hillslope morphologies would be useful in modeling the landscape evolution.

[21] We conclude that morphological decomposition of nonnetwork space into NODs facilitates new measures based on the general statistical relationships and probability distribution functions of the number of NODs and their corresponding areas. We argue that these shape-dependent measures, which are useful to capture the basic dissimilarities between Hortonically similar basins and to adequately characterize the Hortonian and non-Hortonian basin [e.g., *Scheidegger*, 1967] morphologies, are better indicators than Hortonian-based measures.

[22] Intuitively, the hypotheses are that (1) the involved morphologic process in a circular nonnetwork space is different from that of an irregular nonnetwork space and (2) rate of erosion would be relatively lesser in the connected components with higher degree of convexity. In turn, the number distribution functions of NODs would provide insights to explore links with morphologic organization of hillslopes and erosion laws. In order to quantify the basic differences in terms of geomorphic process and landscape response to perturbation due to tectonic and/or climatic settings, shape-dependent measures are particularly useful. This provides an additional important procedure for shape-based classification of landscape. A broader implication is that the nonnetwork spaces within basins with lesser relief ratio (e.g., tidal basins and braided channels) can be better quantified through these shape-based measures. This approach has important yet unexplored implications for how hillslopes can be classified on the basis of geometric organization in a three-dimensional space. Further implications of such a classification would provide insightful ideas toward exploring links between quantitative results and the morphological processes of basins.

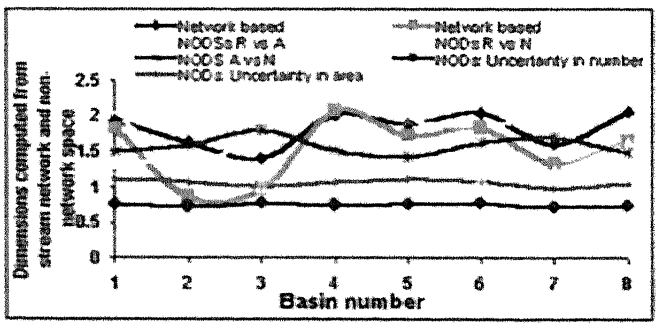

Figure 10. Basin number versus varied dimensions derived from morphometry of networks and nonnetwork spaces. See color version of this figure in the HTML.

[23] **Acknowledgments.** This work was supported in part by MMU internal research grant PR/2003/0273. We gratefully acknowledge Bellie Sivakumar and an anonymous reviewer for providing insightful and helpful recommendations that have improved the paper.

References

Anderson, R. S. (1994), Evolution of the Santa Cruz Mountains, California, through tectonic growth and geomorphic decay, *J. Geophys. Res.*, *99*, 20,161–20,174.

Arenas, A. L., L. Danon, A. Diaz-Guilera, P. M. Gleiser, and R. Guimera (2004), Community analysis in social networks, *Eur. Phys. J. B*, *38*(2), 373–380.

Beer, T., and M. Borgas (1993), Horton's laws and the fractal nature of streams, *Water Resour. Res.*, *29*(5), 1457–1487.

Dodds, P. S., and D. H. Rothman (2001), Geometry of river networks II Distributions of component size and number, *Phys. Rev. E*, *63*, 016116, doi:10.1103/PhysRevE.63.016116.

Dodds, P. S., and J. S. Weitz (2002), Packing of limited growth, *Phys. Rev. E*, *65*, 056108, doi:10.1103/PhysRevE.65.056108.

Dodds, P. S., and J. S. Weitz (2003), Packing-limited growth of irregular objects, *Phys. Rev. E*, *67*, 016117, doi:10.1103/PhysRevE.67.016117.

Fernandes, N. F., and W. E. Dietrich (1997), Hillslope evolution by diffusive processes: The timescale for equilibrium adjustments, *Water Resour. Res.*, *33*, 1307–1318.

Gupta, V. K., and S. Veitzer (2000), Random self-similar networks and derivations of Horton-type relations exhibiting statistical simple scaling, *Water Resour. Res.*, *36*, 1033–1048.

Horton, R. E. (1945), Erosional development of stream and their drainage basin: hydrological approach to quantitattive morphology, *Bull. Geophys. Soc. Am.*, *56*, 275–370.

Howard, A. D. (1990), Theoretical model of optimal drainage networks, *Water Resour. Res.*, *26*, 2107–2117.

Howard, A. D. (1994), A detachment-limited model of drainage basin evolution, *Water Resour. Res.*, *30*, 2261–2285.

Karlinger, M. R., T. M. Over, and B. M. Troutman (1994), Relating thin and fat-fractal scaling of river-network models, *Fractals*, *2*(4), 557–565.

Kirchner, J. W. (1993), Statistical inevitability of Horton's laws and the apparent randomness of stream channel networks, *Geology*, *21*, 591–594.

Kirkby, M. J. (1971), Hillslope process-response models based on the continuity equation, *Inst. Br. Geogr. Spec. Publ.*, *3*, 15–30.

Koons, P. O. (1989), The topographic evolution of collisional mountain belts: A numerical look at the Southern Alps, New Zealand, *Am. J. Sci.*, *289*, 1041–1069.

LaBarbera, P., and R. Rosso (1987), The fractal geometry of river networks, *Eos Trans. AGU*, *68*(44), 1276.

Lian, T. L., P. Radhakrishnan, and B. S. D. Sagar (2004), Morphological decomposition of sandstone pore-space: Fractal power-laws, *Chaos Solitons Fractals*, *19*(2), 339–346.

Mandelbrot, B. B. (1982), *Fractal Geometry of Nature*, W. H. Freeman, New York.

Manna, S. S., and H. J. Herrmann (1991), Precise determination of the dimension of Appollonian packing and space filling bearings, *J. Phys. A Math. Gen.*, *24*, L481–490.

Marani, A., R. Rigon, and A. Rinaldo (1991), A note on fractal channel network, *Water Resour. Res.*, *27*, 3041–3049.

Maritan, A., A. Rinaldo, R. Rigon, A. Giacomatti, and I. Rodriguez-Iturbe (1996a), Scaling laws for river networks, *Phys. Rev. E*, *53*, 1510–1515.

Maritan, A., F. Coloairi, A. Flammini, M. Cieplak, and J. R. Banavar (1996b), Universality classes of optimal channel networks, *Science*, *272*, 984–986.

Maritan, A., R. Rigon, J. R. Banavar, and A. Rinaldo (2002), Network allometry, *Geophys. Res. Lett.*, *29*(11), 1508, doi:10.1029/2001GL014533.

Matheron, G. (1975), *Random Sets and Integral Geometry*, John Wiley, Hoboken, N. J.

Mehta, A. P., C. Reichhardt, C. J. Olson, and F. Nori (1999), Topological invariants in microscopic transport on rough landscapes: Morphology, hierarchical structure, and Horton analysis of river like networks of vortices, *Phys. Rev. Lett.*, *82*, 3641–3644.

Moglen, G. E., and R. L. Bras (1995), The effect of spatial heterogeneities on geomorphic expression in a model of basin evolution, *Water Resour. Res.*, *31*, 2613–2623.

Montgomery, D. R., and W. E. Dietrich (1988), Where do channels begin?, *Nature*, *336*, 232–234.

Montgomery, D. R., and W. E. Dietrich (1994), Landscape disection and draianage area-slope thresholds, in *Processes Models and Theoretical Geomorphology*, edited by M. J. Kirkby, pp. 224–246, John Wiley, Hoboken, N. J.

Nikora, V. I., and V. B. Sapozhnikov (1993), River network fractal geometry and its computer simulation, *Water Resour. Res.*, *29*, 3569–3575.

Olson, C. J., C. Reichhardt, and F. Nori (1998), Fractal networks, braiding channels, and voltage noise in intermittently flowing rivers of quantized magnetic flux, *Phys. Rev. Lett.*, *80*, 2197–2200.

Peckham, S., and V. Gupta (1999), A reformulation of Horton's laws for large river networks in terms of statistical self-similarity, *Water Resour. Res.*, *35*, 2763–2777.

Radhakrishnan, P., T. L. Lian, and B. S. D. Sagar (2004), Estimation of fractal dimension through morphological decomposition, *Chaos Solitons Fractals*, *21*(3), 563–572.

Rigon, R., A. Rinaldo, I. Rodríguez-Iturbe, R. L. Bras, and E. Ijjasz-Vasquez (1993), Optimal channel networks: A framework for the study of river basin morphology, *Water Resour. Res.*, *29*, 1635–1646.

Rinaldo, A., I. Rodriguez-Iturbe, R. L. Bras, and E. Ijjasz-Vasquez (1993), Self-organized fractal river networks, *Phys. Rev. Lett.*, *70*, 822–826.

Rodriguez-Iturbe, I., and A. Rinaldo (1997), *Fractal River Basins: Chance and Self-Organization*, Cambridge Univ. Press, New York.

Roering, J. J., J. W. Kirchner, and W. E. Dietrich (1999), Evidence for nonlinear, diffusive sediment transport on hillslopes and implications for landscape morphology, *Water Resour. Res.*, *35*, 853–870.

Sagar, B. S. D. (1996), Fractal relations of a morphological skeleton, *Chaos Solitons Fractals*, *7*(11), 1871–1879.

Sagar, B. S. D., and L. Chockalingam (2004), Fractal dimension of non-network space of a basin, *Geophys. Res. Lett.*, *31*(12), L12502, doi:10.1029/2004GL019749.

Sagar, B. S. D., and T. L. Tien (2004), Allometric power-law relationships of Hortonian fractal digital elevation model, *Geophys. Res. Lett.*, *31*(6), L06501, doi:10.1029/2003GL019093.

Sagar, B. S. D., C. Omoregie, and B. S. P. Rao (1998), Morphometric relations of fractal-skeletal based channel network model, *Discrete Dyn. Nat. Soc.*, *2*, 72–87.

Sagar, B. S. D., D. Srinivas, and B. S. P. Rao (2001), Fractal skeletal based channel networks in a triangular initiator basin, *Fractals*, *9*(4), 429–437.

Scheidegger, A. A. (1967), A stochastic model for drainage patterns into an intramontane trench, *Bull. Assoc. Sci. Hydrol.*, *12*, 15–60.

Serra, J. (1982), *Mathematical Morphology and Image Analysis*, Elsevier, New York.

Shreve, R. L. (1967), Infinite topologically random channel networks, *J. Geol.*, *75*, 178–186.

Strahler, A. N. (1957), Quantitative analysis of watershed geomorphology, *Eos Trans. AGU*, *38*(6), 913–920.

Takayasu, H. (1990), *Fractals in Physical Sciences*, Manchester Univ. Press, New York.

Tarboton, D. G., and R. L. Bras (1992), A physical basis for drainage density, *Geomorphology*, *5*, 59–76.

Tarboton, D. G., R. L. Bras, and I. Rodriguez-Iturbe (1988), The fractal nature of river networks, *Water Resour. Res.*, *24*, 1317–1322.

Tokunaga, E. (1984), Ordering of divide segments and law of divide segment numbers, *Trans. Jpn. Geomorphol. Union*, *5*, 71–77.

Turcotte, D. L. (1997), *Fractals in Geology and Geophysics*, Cambridge Univ. Press, New York.

Whipple, K. X., and G. Tucker (1999), Dynamics of the stream power river incision model: Implications for height limit of mountain ranges, landscape response time scales, and research needs, *J. Geophys. Res.*, *104*, 17,661–17,674.

Willgoose, G. R., R. L. Bras, and I. Rodriguez-Iturbe (1991), The relationship between catchment and hillslope properties: Implications of a catchment evolution model, *Geomorphology*, *5*, 21–38.

L. Chockalingam, Faculty of Information Science and Technology, Melaka Campus, Multimedia University, Jalan Ayer Keroh Lama, 75450, Melaka, Malaysia.

B. S. Daya Sagar, Faculty of Engineering and Technology, Melaka Campus, Multimedia University, Jalan Ayer Keroh Lama, 75450, Melaka, Malaysia. (bsdaya.sagar@mmu.edu.my)